LEMAC: LTF-EPFL Miniature Atomic Clock Demonstrator Performance Evaluation

C. Affolderbach[1], M. Pellaton[1], Y. Su[2], W. Moreno[1], E. Batori[1], M. Violetti[2,3], A. K. Skrivervik[2], G. Mileti[1]

[1]*Laboratoire Temps-Fréquence, Université de Neuchâtel, Neuchâtel, Switzerland*
[2]*Microwave and Antennas Group, École Polytechnique Fédérale de Lausanne (EPFL),Lausanne, Switzerland*
[3] *Fondazione Toscana Life Sciences, Siena, Italy*

Email : christoph.affolderbach@unine.ch, anja.skrivervik@epfl.ch, gaetano.mileti@unine.ch

***Abstract*— We report on the performance evaluation of the LEMAC miniature atomic clock, based on the optical-microwave Double-Resonance (DR) scheme, implementing a micro-fabricated Rb vapor cell held inside a custom-designed micro-loop-gap microwave resonator (µ-LGR) and a low-power laser source. The clock stability is $1\cdot10^{-11}\ \tau^{-1/2}$ (τ=1 to 100 s) and $4\cdot10^{-12}$ at one day, with low drift of $2\cdot10^{-13}$ /day.**

Keywords—miniature atomic clock, double resonance, Rubidium, microcell, loop-gap resonator,

I. Introduction

Miniature or Chip-Scale Atomic Clocks (CSAC) [1, 2] combine 10^{-11}-level frequency stabilities over several hours timescale with small volume and low power consumption, and have become well-established references for e.g. underwater prospection or holdover applications [3]. Further improved miniature atomic clocks with target specifications aiming beyond current CSAC performances, namely with short-term stability of $1\cdot10^{-10}$ to $1\cdot10^{-11}\ \tau^{-1/2}$ (τ=1 to 100 s) and a long-term frequency drift of < $1\cdot10^{-11}$ to $1\cdot10^{-12}$ /day, are of high interest for emerging applications in the fields of positioning, navigation and timing (PNT) as well as secure telecommunication.

Here we report on the performance evaluation of the LEMAC miniature atomic clock, whose design And development status was presented at the 2022 EFTF conference [4]. In contrast to the majority of reported CSAC that are based on the Coherent Population Trapping (CPT) approach, the LEMAC clock is based on the optical-microwave Double-Resonance (DR) scheme [5, 6] such as to exploit the DR potential for improved short-term stability. In view of small clock volume and power consumption, the LEMAC clock uses a micro-fabricated Rb vapor cell held inside a custom-designed micro-loop-gap microwave resonator (µ-LGR) [7] and a low-power laser source.

II. Clock Description

The highly simple DR scheme implemented in the LEMAC clock assures both a high signal contrast (thus superior short-term clock stability) as well as low light-shift effects, which otherwise could compromise long-term clock stability in alternative schemes such as CPT. The basic clock scheme is depicted in Fig. 1a. A low-power laser diode emits light at the ^{87}Rb D1 line at 975 nm, serving for optical pumping of the ^{87}Rb ground states, see Fig. 1b. Microwave radiation is applied to the ^{87}Rb atoms held in the micro-fabricated vapor cell (containing natural Rb isotopic mixture and a N_2-Ar buffer-gas mixture) [8] via a custom-made µ-LGR and samples the ^{87}Rb $5S_{1/2}$ ground state $|F=1, m_F=0\rangle \leftrightarrow |F=2, m_F=0\rangle$ "clock transition" that serves as atomic reference for stabilizing the clock's output frequency. The laser frequency is stabilized to the optical Rb atomic transition using the signal from the same microcell, encoded in the high-frequency (≈ 70 kHz) part of the photodetector signal.

This activity was conducted and was funded under the Navigation Innovation and Support Program (NAVISP) of the European Space Agency (ESA), to support innovation and competitiveness in the field of Position, Navigation and Time (ESTEC contract nr 4000129974). The views expressed in this document are those of the authors and cannot be taken to reflect the official opinion of the European Space Agency.

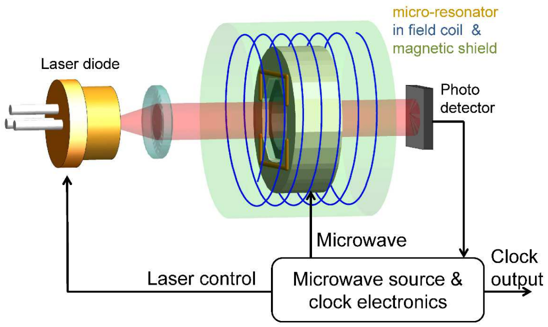

(a)

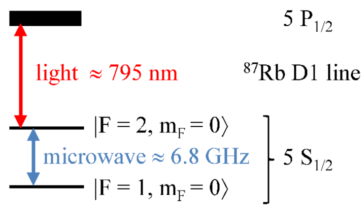

(b)

Fig. 1. (a) Simplified block scheme of the LEMAC Clock. (b) atomic interrogation scheme with optical pumping on the ^{87}Rb D1 line.

A key development of this work is the tuning-free µ-LGR [9] that was entirely redesigned for this LEMAC clock development, as described in a separate proceedings paper of this conference [10]. This tuning-free µ-LGR (volume < 0.65 cm^3) is based on a stack of micro-fabricated planar PCBs made from FR4 substrate and assures operation at the precise ^{87}Rb resonance frequency as well as a highly uniform microwave field across the entire Rb microcell (high Field

Orientation Factor [7] of FOF = 0.75), even in view of manufacturing tolerances, for better production yield. A photograph of the µ-LGR is shown in Fig. 2b and details on this development can be found in [9] and [10].

The overall Physics Package (PP) of the LEMAC clock demonstrator is shown in Fig. 2a. The µ-LGR with the Rb microcell is placed inside a magnetic C-field coil and magnetic shielding, which altogether constitute the Resonator Module (RM). The laser diode is placed inside the brownish thermal cover and constitutes the Laser Source (LS). The both the µ-LGR holding the microcell and the laser diode are temperature controlled using electric heaters and control loops (control electronics not shown). A Power Monitoring module (PM) placed between the LS and the RM picks off a small portion of the laser light in for optical intensity stabilization by acting on the laser diode's temperature. The Detector Module (DM) placed behind the RM uses a photodetector to measure the light intensity transmitted through the RM. The high-frequency part (≈ 70 kHz) of this signal is used to stabilize the laser frequency to the microcell inside the RM, and its low-frequency part (≈ 200 Hz) carries the clock signal and is used to steer the clock quartz' and thus the clock output frequency. The overall size of the black PP enclosure seen in Fig. 2a is 86 x 86 x 48 mm^3 (< 360 cm^3), currently larger than necessary due to the sub-D connectors connecting to the clock electronics (made from standard laboratory electronics, not shown).

III. Demonstrator Performance

Figure 3 shows a typical optical clock signal from the LEMAC demonstrator, obtained at a cell temperature of

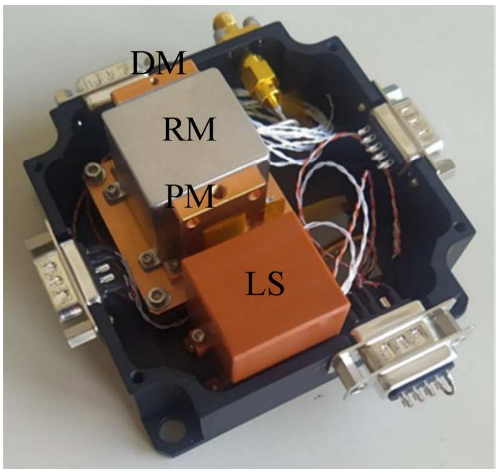

(a)

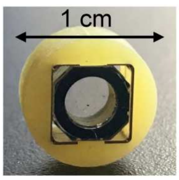

(b)

Fig. 4. (a) Photo of the LEMAC Photo of the LEMAC clock demonstrator. The overall size of the black PP enclosure is 86 x 86 x 48 mm^3 (< 360 cm^3), with the Laser Source (LS) and atomic Resonator Module (RM) as main parts. (b) close-up photograph of the µ-LGR holding the microcell, as implemented in the clock's RM.

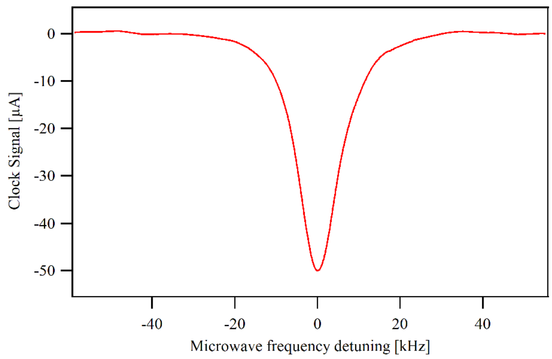

Fig. 2. Optimized clock signal of the measured on the LEMAC clock demonstrator.

99°C, 10 µW of laser power and 100 µW of microwave power. The signal has a linewidth of FWHM ≈ 11 kHz, an amplitude of 52 nA at a background level of 1 µA (in terms of photodetector current) and a detection noise around 1 pA·Hz$^{-1/2}$. From this data we deduce an expected signal-to-noise (SNR) limit for the clock's short-term stability of $\sigma_{SNR} \approx 2.5 \cdot 10^{-11}\ \tau^{-1/2}$.

The measured clock frequency is shown in Fig. 4a, for a clock run of 1-week duration. No drift was removed from the frequency data of Fig. 4a and the overall frequency drift of this measurement amounts to only 2.3·10^{-13} /day. The Allan deviation plot derived from this data and shown in Fig. 4b displays a short-term clock stability of 2.2·10^{-11} $\tau^{-1/2}$ at 1 to 100 s and a long-term stability of ≈ 4·10^{-12} at 1 day.

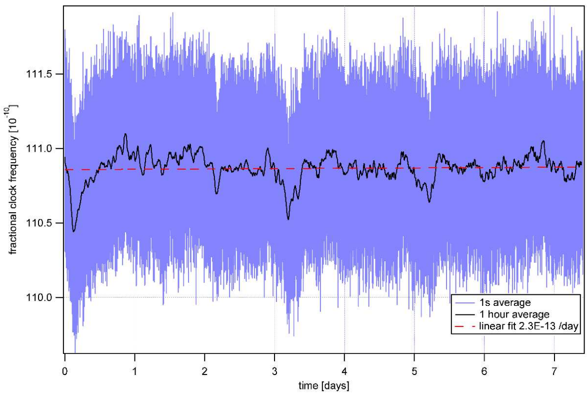

(a)

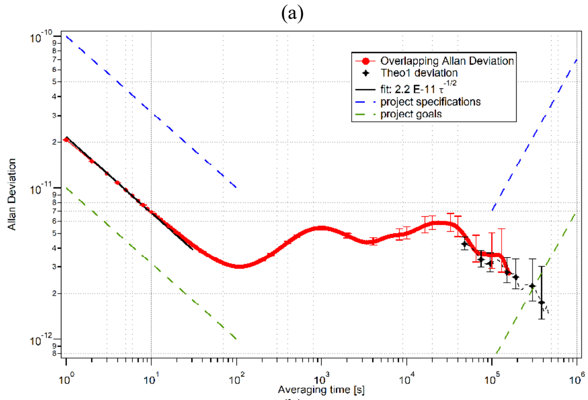

(b)

Fig. 3. (a) clock frequency data recorded for a 1-week duration. No drift removal was performed on this data. (b) clock stability in terms of Allan deviation, calculated from the freuqency data of panel (a).

TABLE I. LONG-TERM CLOCK STABILITY BUDGET FOR THE LEMAC CLOCK, ESTABLISHED AT $\tau=10^5$ SECONDS (≈ 1 DAY).

Physical effect	Physical parameter	Sensitivity coefficient	Parameter fluctuation at 10^5s	Clock instability contribution at 10^5s
Intensity Light-Shift	Laser intensity	$5.5\cdot10^{-10}$ /µW	$5.4\cdot10^{-4}$ µW	$3.0\cdot10^{-13}$
Frequency Light-Shift	Laser frequency	$9.9\cdot10^{-17}$ /Hz	$3.8\cdot10^{4}$ Hz	$3.7\cdot10^{-12}$
Temperature coefficient	Cell temperature	$8.0\cdot10^{-10}$ /K	$8.0\cdot10^{-4}$ K	$6.4\cdot10^{-13}$
Microwave Power Shift	Microwave power	$7.4\cdot10^{-12}$ /µW	0.2 µW	$1.5\cdot10^{-12}$
2nd order Zeeman shift	C-field	$1.8\cdot10^{-4}$ /T	$1.3\cdot10^{-9}$ T	$2.3\cdot10^{-13}$
Total				$\mathbf{4.1\cdot10^{-12}}$
Measured				$\mathbf{3.6^{+1.5}_{-0.7}\cdot10^{-12}}$

As can be seen, the clock stability corresponds well to the development goals given in the introduction (dashed lines).

A. Short-Term Clock Stability

The measured short-term clock stability of $2.2\cdot10^{-11}$ $\tau^{-1/2}$ is in good agreement with the expected signal-to-noise-limit, indicating a SNR-limited short-term performance. Other effect (such as light-shift) result in limitations to the short-term instability at a negligible level of $< 4\cdot10^{-12}$ $\tau^{-1/2}$.

B. Long-Term Clock Stability

In order to understand the physical effects that limit the clock stability at long-term timescales of one day and beyond, a detailed stability budget was established at a timescale of $\tau = 10^5$ seconds (≈ 1 day), see Table I. All sensitivity coefficients shown were measured on the LEMAC clock under its nominal operating conditions, with exception of the 2nd-order C-field Zeeman shift that was calculated from theory. The laser frequency fluctuation data was taken from [11] while all other parameter fluctuations were measured on the LEMAC clock demonstrator during the tests. We clearly see that the largest and dominant clock instability contribution arises from the frequency light-shift (level of $3.7\cdot10^{-12}$) with the laser frequency stabilized to the Doppler- and collisional-broadened optical reference line from the microcell, followed by the microwave power shift (amounting to $1.5\cdot10^{-12}$, no active microwave power control implemented). The total long-term stability limit of $4.1\cdot10^{-12}$ derived from this budget is in good agreement with the measured stability of $3.6(+1.5/-0.7)\cdot10^{-12}$, given the statistical uncertainty of the experimental Allan deviation data. The long-term clock stability is thus well understood.

IV. CONCLUSIONS

We have measured and metrologically analyzed the stability performance of the LEMAC clock, a miniature atomic clock based on the double-resonance scheme and a custom-made, tuning-free µ-LGR as miniature microwave resonator. The short-term clock stability is ≈ $2.2\cdot10^{-11}$ $\tau^{-1/2}$, limited by the signal-to-noise limit of the optical detection, and the long-term stability is ≈ $4\cdot10^{-12}$ at 1 day, with low drift of ≈ $2\cdot10^{-13}$ /day from a very simple miniature clock setup. The detailed meteorological budget established shows that the main current limitation to the 1-day stability arises from the frequency light-shift, that can be further reduced by implementing pulsed Ramsey interrogation (µ-POP scheme) on the LEMAC clock [12].

ACKNOWLEDGMENT

We thank P. Waller (ESA-ESTEC) for following the project and for fruitful technical exchanges. We also thank P. Scherler and F. Gruet of Unine-LTF for valuable technical assistance, and M. Veljovic (formerly EPFL-MAG) for contributions to the early phase of the project.

REFERENCES

[1] S. Knappe, "MEMS atomic clocks," in Comprehensive Microsystems, Y. B. Gianchandani, O. Tabata, and H. Zappe, eds., (Elsevier, 2008), pp 571–612.

[2] R. Lutwak et al., "The Chip-Scale Atomic Clock – Prototype Evaluation", proceedings of the 39th Annual Precise Time and Time Interval (PTTI) Meeting (2007), p. 269 – 290.

[3] A. T. Gardner and J. A. Collins, "A Second Look at Chip Scale Atomic Clocks for Long Term Precision Timing - Four Years in the Field", proceedings of the OCEANS 2016 MTS/IEEE Monterey conference, 19-23 Sept. 2016.

[4] M. Pellaton et al., "LEMAC: LTF-EPFL Miniature Atomic Clock: current status", Proceedings of the joint EFTF and IFCS 2022, paper 5066, 2022.

[5] J. Camparo, "The rubidium atomic clock and basic research", Phys. Today **60**, 33 (2007).

[6] T. Bandi, C. Affolderbach, C. Stefanucci, F. Merli, A. K. Skrivervik, G. Mileti, "Compact high-performance continuous-wave double-resonance rubidium standard with 1.4x10^{-13} $\tau^{-1/2}$ stability", IEEE Transactions on Ultrasonics, Ferroelectrics, and Frequency Control **61**, 1769 – 1778 (2014).

[7] M. Violetti et al., "The Micro Loop-Gap Resonator: A Novel Miniaturized Microwave Cavity for Double-Resonance Rubidium Atomic Clocks", IEEE Journal of Sensors **14**, 3193 - 3200 (2014).

[8] Y. Pétremand et al., "Microfabricated rubidium vapour-cell with a thick glass core for small scale atomic clock applications", Journal of Micromechanics and Microengineering **22**, 025013 (2012).

[9] Y. Su et al., "Mode Suppression and Homogeneous Field Bandwidth Enhancement of a Tuning-Free Micro-Loop-Gap Resonator Using FR4 for Chip-Scale Rubidium Clock", IEEE Transactions on Microwave Theory and Techniques **72**(6), 3711-3721 (2024).

[10] Y. Su et al., "Micro-Loop-Gap Microwave Resonator Development for the LEMAC LTF-EPFL Miniature Atomic Clock", in Proceedings

of the 37th European Frequency and Time Forum EFTF, paper 2121, 2024. In press.

[11] C. Affolderbach, Ch. Andreeva, S. Cartaleva, G. Mileti, and D. G. Slavov, "Frequency stability comparison of diode lasers locked to Doppler and sub-Doppler resonances", Proc. SPIE 5449, Eighth International Conference on Laser and Laser Information Technologies, (21 June 2004).

[12] E. Batori et al., “µPOP Clock: A Microcell Atomic Clock Based on a Double-Resonance Ramsey Scheme”, Physical Review Applied **18**, 054039 (2022).